

## Review Article

Nigel R. Farrar\*, Bruno M. La Fontaine, Igor V. Fomenkov and David C. Brandt

# Advances in EUV light sources

**Abstract:** Extreme ultraviolet (EUV) lithography has emerged as the preferred choice for high-volume manufacturing, now that immersion ArF reaches its limits. Light source power is a key driver to achieve the throughput required for successful adoption of extreme ultraviolet lithography (EUVL). Cymer has developed a laser-produced plasma source based on a high-power CO<sub>2</sub> drive laser exciting tin targets to emit 13.5 nm light. Five sources are currently installed at chipmaker fabs and are being used for process development. The power output of the fielded source configuration is currently 20 W, lower than required for manufacturing introduction. The technology for scaling up power is under development, focusing on increasing the conversion efficiency and collection efficiency of the source. Increasing drive laser power to 17 kW has allowed the demonstration of EUV power of nearly 50 W, with paths identified for further scaling to 100 W. An additional focus on product reliability has driven the availability up to 70%, primarily through extending the collector mirror lifetime.

**Keywords:** collector; droplet generator; EUV lithography; EUV source; laser-produced plasma.

---

\*Corresponding author: Nigel R. Farrar, Cymer Inc., 17075 Thornmint Court, San Diego, CA 92127, USA, e-mail: Nigel\_Farrar@Cymer.com

Bruno M. La Fontaine, Igor V. Fomenkov and David C. Brandt: Cymer Inc., 17075 Thornmint Court, San Diego, CA 92127, USA

## 1 Introduction

EUV lithography is the leading prospect for extending the resolution beyond the performance currently available using ArF immersion and double patterning. The resolution capability of extreme ultraviolet lithography (EUVL) is already clear from early imaging tests on pre-production scanners [1]. Production viability will be determined by the productivity and maturity of these systems. Additional challenges associated with mask defect reduction and resist resolution, sensitivity, and line-width roughness

also require work to achieve an acceptable high-volume manufacturing capability.

Most attention is being focused on the development of a robust, high-power light source that will enable EUVL to realize the throughput necessary to achieve the cost targets required for it to be introduced into production. Two EUV source architectures have been under consideration. Laser produced plasma (LPP) sources have been studied for about 20 years and are the most likely architecture to provide the continued power scaling requirements that are expected [2–5]. The alternative architecture, discharge-produced plasma (DPP) has significant challenges with power scaling, primarily due to greater difficulty in handling the large heat loads within the system. Power scaling in a LPP architecture is expected to be achieved primarily through scaling up of the input laser power. For a 100-wph throughput, using 15 mJ/cm<sup>2</sup> resist, it is expected that about 250 W of source power will be required for the full-scale adoption of EUVL.

## 2 Cymer LPP source architecture

Cymer's source architecture currently focuses a high power, pulsed CO<sub>2</sub> laser on small droplets of molten tin, which creates a highly ionized plasma that emits at the 13.5-nm wavelength required for EUV lithography. Further details can be found in several past publications [6–11]. A schematic of the overall source is shown in Figure 1. Typically, the CO<sub>2</sub> laser is installed in the customer subfab, and the laser beam is transmitted to the source vessel within the scanner by a totally enclosed and interlocked beam transport system. The RF generators and heat exchangers for the laser are also installed in the subfab but are not shown in Figure 1. The beam transport system is designed for adjustable length and with multiple turning mirrors to allow for flexible positioning of the laser relative to the scanner location in the fab. The laser beam is expanded during transmission to the vessel to reduce the heat load on the transport optics.

A schematic of the source vessel is shown in Figure 2. This vessel is located within the scanner enclosure in the fab. The beam enters the vessel through a central hole in the collector mirror to impinge on the tin droplets at one focus

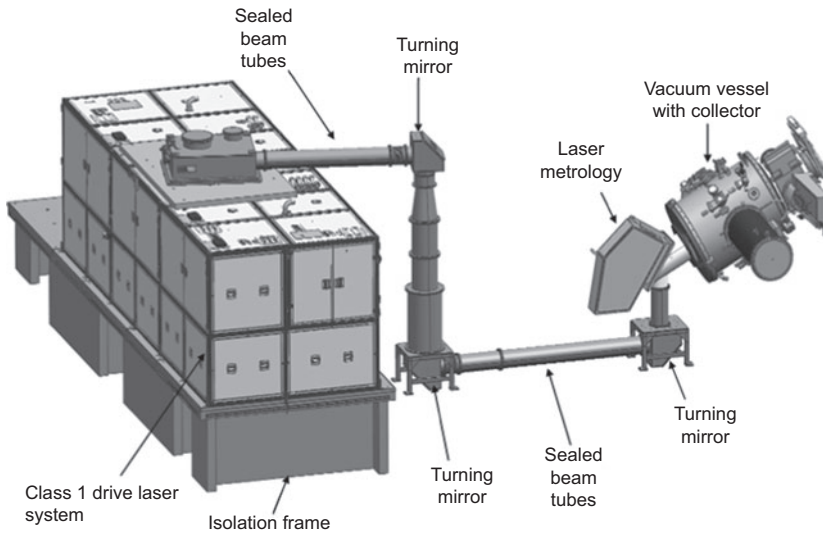


**Figure 1** Schematic of a LPP source.

of the elliptical mirror. The laser beam is focused by a lens to a diffraction limited spot size of about  $100\ \mu\text{m}$ . The laser vaporizes the tin and creates a plasma, which emits radiation isotropically over a range of wavelengths, including the desired  $13.5\ \text{nm}$ . The drive laser has multiple stages of amplification to achieve the current  $17\text{-kW}$  output, with plans to scale to  $30\ \text{kW}$  when a higher source power is required. It is operated at repetition rates between  $40$  and  $60\ \text{kHz}$ .

The mirror collects and refocuses the  $13.5\text{-nm}$  radiation to the second focus of the ellipse, which is the intermediate focus point and entry aperture to the scanner. The mirror coating is a silicon/molybdenum multilayer designed to select a narrow band of wavelengths around  $13.5\ \text{nm}$  and is similar to the coatings on the illuminator and projection optics in the scanner. The pulses of light from the laser are synchronized with a stream of molten tin droplets, which are emitted from the droplet generator at about  $60\ \text{m/s}$ . Both the laser beam and droplets are timed and positioned

using feedback and control to accurately center the pulse on each droplet. Droplet size is currently  $30\ \mu\text{m}$ .

One key advantage of the LPP source architecture is that the hot plasma is isolated in space at some distance from critical vessel components [12]. This results in heat loads in the system that are orders of magnitude less than those in a DPP source and are significantly more manageable. The LPP architecture also results in a small plasma size, which provides for more efficient collection of the light and more effective creation of illumination shapes for higher resolution imaging.

The key attributes of an efficient EUV source are high conversion efficiency and high collection efficiency. Conversion efficiency is the percentage of incoming  $\text{CO}_2$  laser energy that is converted into an in-band  $13.5\ \text{nm}$  radiation. This depends on the laser wavelength, the choice of target material, and the effectiveness of the beam/droplet targeting system. Radiation is emitted in all directions so it is important to have a high collection efficiency that maximizes the percentage of  $13.5\ \text{nm}$  light that is redirected through the intermediate focus aperture. In the LPP architecture, the ability to collect a large solid angle of light is not constrained by electrodes or other vessel components that may restrict the collection angle. In addition, the open geometry allows the use of a multilayer mirror at near-normal incidence, which provides high reflectivity and wavelength selectivity.

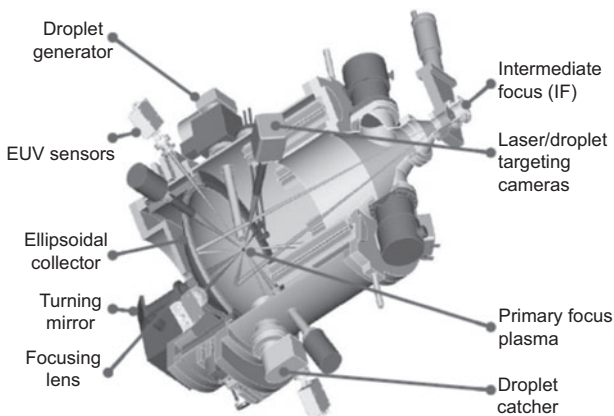


**Figure 2** Schematic of a pilot source vessel, showing key components such as droplet generator, collector, and final focusing lens.

### 3 Power scaling

As discussed above, the key attributes of a source architecture for flexible power scaling are input power scalability,

conversion efficiency, and collection efficiency. Currently, the maximum laser output power, with good beam quality, is ~17 kW. This needs to be increased to ~20 kW, along with other technology development discussed below, to reach an EUV output power of ~100 W. Further increases to ~30 kW are expected to be required to reach future targets of 250–350 W.

Power output is primarily achieved by maximizing the conversion efficiency from drive laser power to EUV output power. During early work on LPP sources, several target materials expected to show emission in the 13- to 15-nm wavelength range were investigated using different drive lasers with various emission wavelengths. The results from testing on solid targets are shown in Table 1. Here, it can be seen that the combination of CO<sub>2</sub> light, at 10 μm wavelength, and a tin target provided the highest conversion efficiency of up to 5%. Investigation of whether a higher conversion efficiency could be obtained from other materials, such as alloys of tin, indium, and gallium, was carried out using a CO<sub>2</sub> drive laser and flat targets. An additional purpose of this study was to investigate whether a lower melting point alloy with good conversion

efficiency would be a suitable candidate to replace tin and simplify the design of the droplet generator.

Figure 3 shows the EUV spectra for pure tin and indium, in addition to a tin-indium alloy (48/52), tin-gallium alloy (8/92), and tin-indium-gallium alloy (16/22/62). The materials containing indium showed conversion efficiency peaks at 14.5 nm, which is not suitable for use with conventional silicon-molybdenum multilayer mirrors. Conversion efficiency at 13.5 nm was measured with an in-band EUV detector; the numbers at 14.5 nm were predicted based on measured spectra and conversion efficiency at 13.5 nm. No materials showed better overall performance than pure tin. The tin-gallium alloy had a lower melting temperature (21°C) but only half the conversion efficiency, and pure indium had equivalent conversion efficiency and a low melting point (157°C) but at 14.5 nm.

Conversion efficiency measurement results on flat solid targets need to be reproduced using molten droplets in order to be used in a production source. The use of droplets is required in order to limit the amount of tin debris within the vessel and reduce the risk of contamination of the collector mirror resulting in a loss of reflectivity. Obtaining high conversion efficiency using a droplet stream is challenging because it requires excellent control of the focus position of the drive laser beam and precise synchronization of the timing and position of the droplets and laser pulses.

In addition, since the diffraction limited spot size of the laser is larger than practical droplet sizes of about 30 μm, a prepulse technique is under development to expand the droplet before the main laser pulse in order

	Xenon	Tin	Lithium
Excimer (351 nm)	–	0.5–1.0%	2.0–2.5%
Solid state (1064 nm)	0.5–1.0%	2.0–2.5%	2.0–2.5%
CO <sub>2</sub> (10 600 nm)	0.5–1.0%	4.0–5.0%	1.0–1.5%

**Table 1** Conversion efficiency of various target materials with different laser excitation wavelengths.

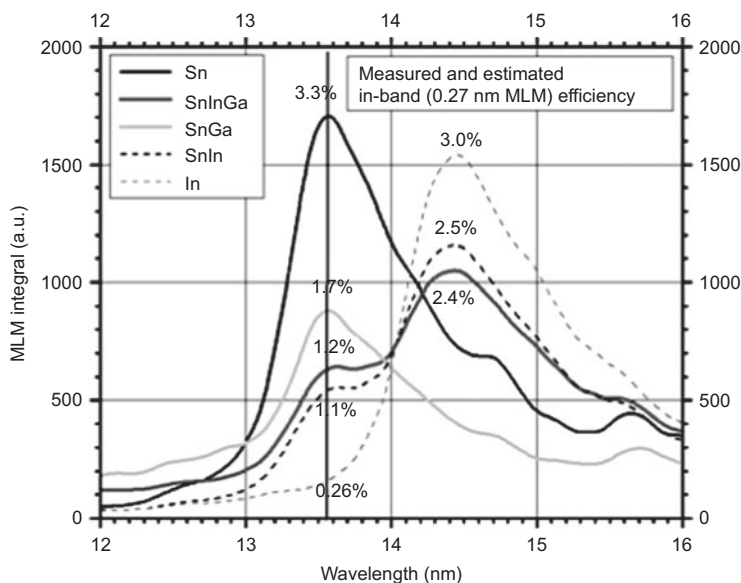


**Figure 3** Measured conversion efficiency for a number of selected target materials.

to maximize the interaction area and coupling of the laser pulse energy with the droplet and increase conversion efficiency. To date, this configuration has produced a conversion efficiency of about 3% and up to 50 W of average output power, at 50 kHz. Average EUV power as a function of duty cycle is shown in Figure 4. In this case, the automated laser beam and droplet position control loops were not active. Manual synchronization of the laser beam and droplets resulted in lower conversion efficiency as duty cycle increased. Power of 90 W within a burst was achieved at a low duty cycle, but this dropped to 60 W at a higher duty cycle due to increasingly difficult synchronization between the laser pulse and droplet, which results in a lower conversion efficiency. Activation of all automated control loops is expected to result in the power output being maintained as the duty cycle increases.

In addition to increasing the drive laser pulse energy, EUV power can also be scaled by increasing the repetition rate. Testing with repetition rates as high as 80 kHz has been carried out. These data showed that an operation above about 60 kHz was possible if droplets adjacent to the target droplet were not affected by the shock front from the plasma generation. However, this requires the droplets to travel at a velocity sufficiently high to maintain a safe separation from plasma effects. Figure 5 shows droplets at a repetition rate of 120 kHz where the effect of the plasma is visible on the droplet following the target droplet. The next droplet is unaffected by the plasma indicating that a 16.6-ms separation, or 60-kHz operation, can be used for power scaling.

Additional measurements of conversion efficiency at an increasing repetition rate were carried out and are shown in Figure 6. The conversion efficiency with prepulse was stable at about 3% up to about 60 kHz but started to tail off at 70 kHz and showed a significant reduction at

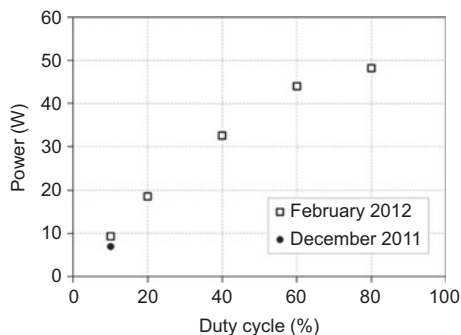


**Figure 4** Average EUV power, as a function of duty cycle, obtained using a laser prepulse.

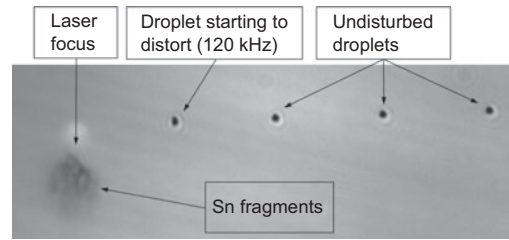


**Figure 5** Image of a stream of 30  $\mu\text{m}$  tin droplet targets, separated by 8.3 ms ( $\sim 500 \mu\text{m}$ ).

80 kHz. Operation at higher repetition rates may be possible by using higher droplet velocity in order to maintain a larger separation and isolate them from any deleterious effects of the expanding plasma.

In these results, the conversion efficiency is still limited by the ability to fully control the laser droplet targeting under all operating conditions and optimize the beam intensity on target. Improvements to the conversion efficiency are expected from improvements to both the droplet trajectory stability and the measurement and control precision. This, in addition to stabilization of the focused laser beam quality, and position and power stability, is expected to increase the conversion efficiency to meet the power scaling roadmap (shown in Table 2).

## 4 Collection efficiency

Collection efficiency is the second key attribute of a high power source. In the LPP architecture, this is primarily determined by the characteristics of the five steradian collector mirrors within the vessel (see Figure 7). The development of manufacturing techniques for the large, high

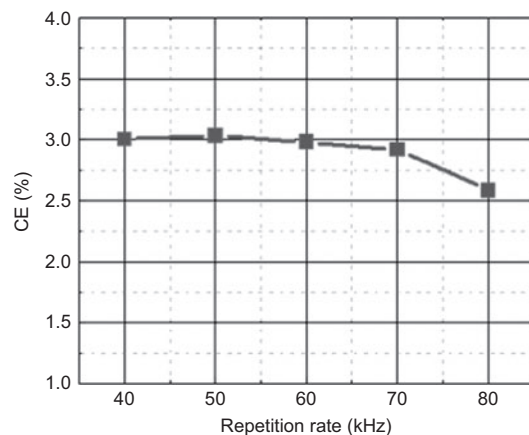


**Figure 6** Measured conversion efficiency as a function of the operating repetition rate.

**EUV source power roadmap**

Source model	HVM I	HVM II	HVM III
Average laser power (kW)	13	29	31
In-band CE (%)	3.0	3.5	4.0
Clean EUV power (W)	105	250	350

**Table 2** LPP EUV source power roadmap.

reflectivity mirror has been underway for some time. As the mirror design is ellipsoidal, with the plasma at one focus and the intermediate focus aperture at the other, the incident angle of light onto the mirror varies with the radius. In order to achieve maximum reflectivity, a graded spacing multilayer is deposited. Development of such coatings has resulted in a maximum reflectivity of about 60% in the center of the mirror and an area weighted average reflectivity of over 50%, with good uniformity and reproducibility, as shown in Figure 8 for several recent collectors.



**Figure 7** LPP collector mirror.

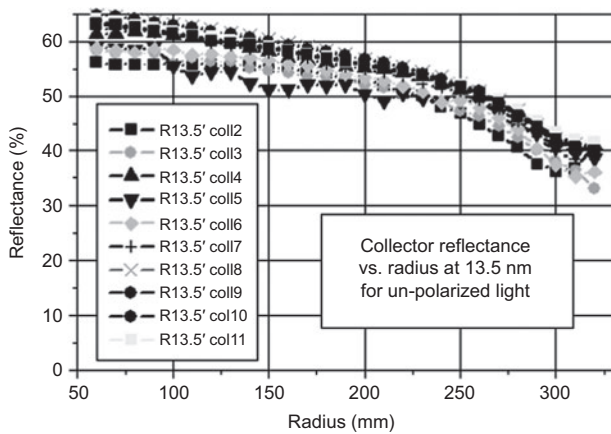


**Figure 8** Reflectivity for several mirrors.

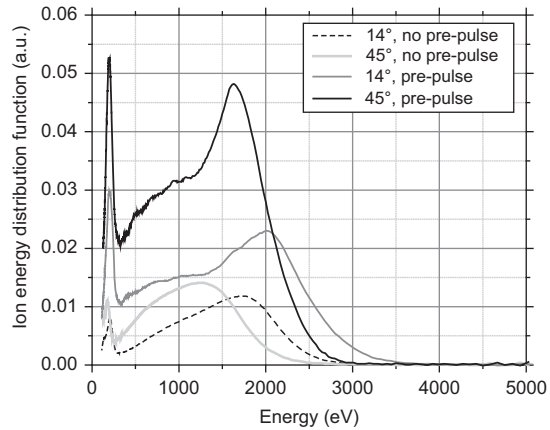


**Figure 9** Ion energy spectra at collection angles of 14° and 45° from the laser beam.

It is also vital that the mirror reflectivity be maintained despite potential contamination from debris from the tin droplets that can reduce reflectivity if allowed to etch or deposit on the mirror surface. Understanding the influence of tin ions and neutrals reaching the collector is important in order to implement an effective mitigation scheme to maintain reflectivity.

Measurements of the ion energy generated during the laser-plasma interaction, at two collection angles (14° and 45°) are shown in Figure 9. The maximum ion energy is 2.5–3.5 keV. The use of prepulse results in an increase in total ion flux, in addition to a shift to higher energy. The high-energy ions could potentially result in sputtering of the collector coating layers. To prevent this, the pilot sources use a hydrogen background gas in the vessel to reduce the number of high-energy ions by gas collision interactions.

The collector lifetime can also be extended by covering the multilayer mirror with a protective coating. Many different types of coatings have been evaluated, and the performance of two such coatings is shown in Figure 10, for sources operating in the field. Both coatings show no change in the initial EUV reflectivity after approximately  $2.8 \times 10^{10}$  pulses in the case of coating A and  $1.1 \times 10^{10}$  pulses in the case of coating B, respectively, with evaluation still ongoing. This is a significant improvement in the coating

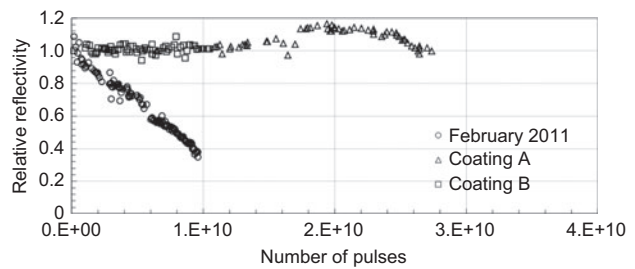


**Figure 10** Recent collector lifetime results from sources in the field.

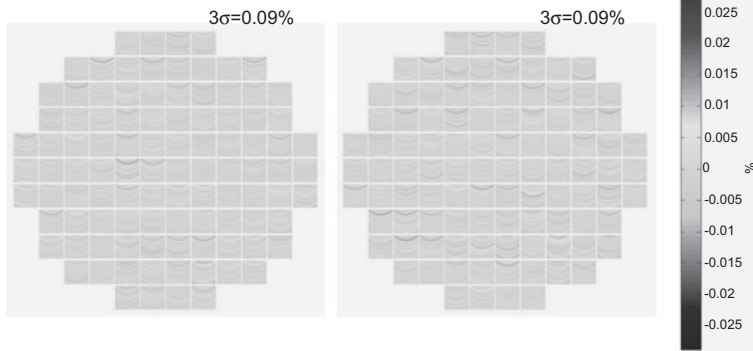


**Figure 11** EUV dose stability at an average power of 20 W.

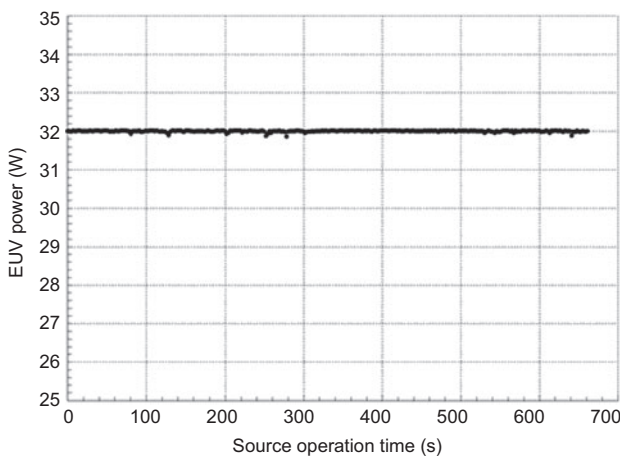


**Figure 12** Average power of 32 W with better than  $\pm 0.5\%$  dose stability.

lifetime compared to 1 year ago where reflectivity had dropped by 10% after only  $2 \times 10^9$  pulses. Further development is in progress to develop coatings, which can achieve the target of 1-year collector lifetime.

The hydrogen gas, which minimizes etching of the mirror, also mitigates a second mechanism, which can potentially shorten the lifetime of the collector. Deposition

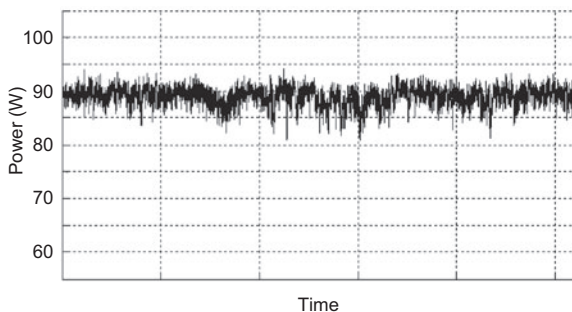


**Figure 13** Burst power of 90 W at 20% duty cycle (18 W average power) using prepulse.

of tin neutral atoms on the surface of the collector can lead to the formation of an EUV absorbing film and loss of reflectivity. Here, hydrogen radicals formed by the interaction of the plasma with the hydrogen gas, can clean or etch tin from the surface of the collector by forming volatile stannane ( $\text{SnH}_4$ ), which is removed by the vacuum pumps. The data in Figure 10 show the effectiveness of the hydrogen gas in mitigating reflectivity loss from both mechanisms.

## 5 Source status

Cymer has now built 10 integrated sources, including one prototype source. Six pilot sources have been delivered to customers, and five have been installed at chipmaker fabs, where they are in daily operation and being used for advanced process development. The other four sources are used in the factory for parallel development in the areas of power scaling, lifetime testing, and reliability improvement.

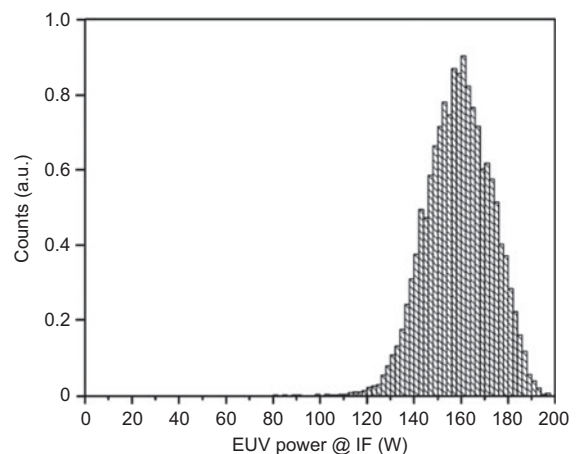


**Figure 14** Demonstration of a 158-W EUV power at a duty cycle of about 3%.

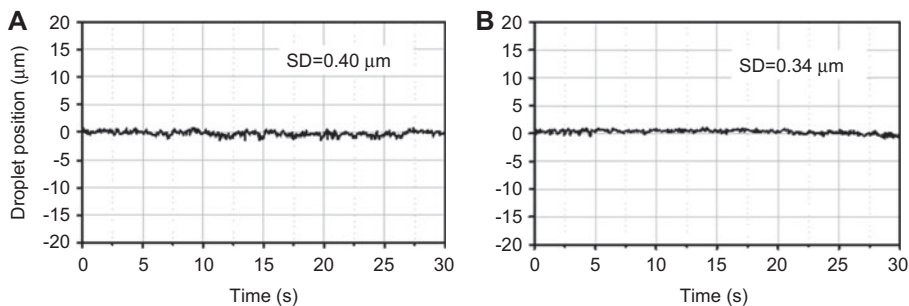


**Figure 15** (A) Day 1 droplet stability. (B) Day 46 droplet stability.

These fully integrated sources are currently capable of producing 20 W of usable average power with closed loop active dose control. For testing at the factory, a scanner simulator allows operation under typical scanner conditions for wafer exposures in a fab. A key performance characteristic is the dose stability of the source, within each exposure field and across wafers. Results are analyzed by examining wafer dose maps, as shown in Figure 11. Typical results show that each exposure field has better than the required  $\pm 0.5\%$   $3\sigma$  dose stability, with more than 99.7% of the simulated exposure fields meeting the dose stability requirements.

Other source configurations have demonstrated higher power. Figure 12 shows a 32-W average dose-controlled power with a higher power laser configuration. Figure 13 shows results from a prepulse configuration, which produced 50 W of average power, but without active dose control at this stage. Advanced developments on an experimental prototype source using a 28-kW peak drive laser power has shown up to 160 W in-burst EUV power output at a low duty cycle (see Figure 14). This technology is in the process of being incorporated into the pilot design and will form the basis for the next generation of higher power sources.

## 6 Availability

The other important aspect of source performance for production worthiness is availability. This has been tracked using SEMI E-10 standards definition and is currently at approximately 70%. Most unavailable time is due to scheduled downtime associated with droplet generator exchanges and collector mirror replacements. Reductions in collector exchange time, together with reducing the frequency of exchange through longer collector lifetime, as discussed above, are the key factors to improved availability.

Currently, a droplet generator contains enough tin to run for about one week. Longer run times are expected through work on larger tin reservoirs, *in situ* refills, and the use of smaller droplets. Testing of new droplet generator-operating

modes has been extended to 46 days without the loss of droplet stability, as shown in Figure 15. Longer run times, faster exchange times, and improved reliability are all expected to reduce the downtime associated with this key module.

Improvements in these two areas, plus enhanced automation of source operation have resulted in increased availability over the last year.

## 7 Summary

LPP EUV light sources are expected to provide the power scaling necessary for the high throughput operation required for EUVL introduction into manufacturing. Fully integrated sources have now been delivered to several chipmaker fabs, where they are being used for process development. Availability has improved steadily after installation with improvements to droplet generator reliability and running time, and increases in the collector mirror lifetime, and now stands at about 70%. Further improvements, particularly in the collector lifetime, are expected to provide further improvements.

At this time, the power output is still lower than the target and technology development to increase power, with plans for field upgrades, are in progress on several additional fully integrated sources. The current source configuration is now capable of operating at 20 W. Using a prepulse configuration, up to 50 W of average power and 90 W of in-burst power has been demonstrated. Once the automation of the laser droplet position controls is included in the prepulse configuration, the average source power is expected to reach power levels of about 100 W. Further scaling of source power through operation at higher drive laser power and higher repetition rates will allow further power scaling to 250–350 W levels, as shown in the roadmap in Table 2, and will enable the introduction of EUVL into high-volume manufacturing.

**Acknowledgements:** The authors acknowledge the many contributions of past and present scientists, engineers, and technicians in the EUV technology program at Cymer. We also thank our colleagues at ASML for many helpful

discussions on various aspects related to the light source operation.

Received June 12, 2012; accepted July 28, 2012

## References

- [1] C. Wagner, J. Bacelar, N. Harned, E. Loopstra, S. Hendriks, et al., Proc. SPIE 7969, 79691F (2011).
- [2] M. Richardson, in 'Extreme Ultraviolet Lithography', Ed. By B. Wu and A. Kumar, Ch. 3, 121–167 (McGraw-Hill, New York, 2009).
- [3] P. D. Rockett, J. A. Hunter, R. Kensek, R. E. Olson, G. D. Kubiak, et al., in OSA Proc. On Soft X-Ray Projection Lithography, 12, 76–79 (1991).
- [4] M. Chaker, B. La Fontaine, C. Y. Cote, J.-C. Kieffer, H. Pepin, et al., J. Vac. Sci. Technol. B 10, 6 (1992).
- [5] R. L. Kauffmann, D. W. Phillion, R. C. Spitzer. Appl. Opt. 32(34), 6897–6900 (1993).
- [6] D. C. Brandt, I. V. Fomenkov, A. I. Ershov, W. N. Partlo, D. W. Myers, et al., Proc. SPIE 7271, 727103 (2009).
- [7] N. R. Böwering, I. V. Fomenkov, D. C. Brandt, A. N. Bykanov, A. I. Ershov, et al., Journal of Micro/Nanolith. MEMS MOEMS 8, 041504 (2009).
- [8] D. C. Brandt, I. V. Fomenkov, A. I. Ershov, W. N. Partlo, D. W. Myers, et al., Dunstan, Proc. SPIE 7636, 76361I (2010).
- [9] I. V. Fomenkov, A. I. Ershov, W. N. Partlo, D. W. Myers, R. L. Sandstrom, et al., Proc. SPIE 7636, 763639 (2010).
- [10] I. V. Fomenkov, A. I. Ershov, W. N. Partlo, D. W. Myers, D. Brown, et al., Proc. SPIE 7969, 796933 (2011).
- [11] K. Nishihara, A. Sunahara, A. Sasaki, M. Nunami, H. Tanuma, et al., Phys. Plasmas 15, 056708 (2008).
- [12] V. Y. Banine, K. N. Koshelev, and G. H. P. M. Swinkels, J. Phys. D: Appl. Phys. 44, 253001 (2011).



Nigel R. Farrar is the Vice President of Lithography Applications at Cymer, Inc., and is a member of its Scientific Advisory Board. He joined Cymer in 1999 and has led activities to identify the critical performance factors for the light source in the microlithography process. Prior to joining Cymer, he spent 15 years at Hewlett Packard working on advanced microlithography technologies. He has authored over 40 technical papers in the field of microlithography process technology. He holds BS and PhD degrees in Physics from the University of Bristol in England.



Bruno LaFontaine has served as the senior director of global EUV lithography applications at Cymer, Inc. since February 2010, where he is responsible for leading the application development for the company's laser produced plasma (LPP) EUV light sources. Involved in the EUV lithography industry since 1992, LaFontaine brings to Cymer nearly a decade of expertise in EUV, light sources, physics and optics. Prior to joining Cymer, LaFontaine held fellow of lithography positions, first at Advanced Micro Devices (AMD) and later at GLOBALFOUNDRIES. Before AMD, LaFontaine held roles at the Lawrence Livermore National Laboratory and Bell Laboratories. Since 2007, LaFontaine has served as conference chair for SPIE, the international society for optics and photonics. He received his bachelor's degree in physics from the Université de Montréal and his masters and doctorate in physics from the Institut National de la Recherche Scientifique.



Igor V. Fomenkov graduated and received his PhD in Physics and Mathematics from the Moscow Institute of Physics and Technology in 1981 and 1986, respectively. He worked as a senior scientist at the Institute of General Physics. His research was conducted in areas of interaction of laser radiation with matter and plasma diagnostics. Since 1992, he has been with Cymer Inc., currently as Fellow, working on research and development of excimer lasers and EUV light sources for microlithography applications.



David Brandt serves as Senior Director of EUV Marketing with nearly two decades of experience in engineering, product development, and marketing. Before leading the program and marketing activities within the EUV development group, Brandt spent the last decade filling several critical roles at Cymer – from managing the company’s international subsidiaries in Taiwan and Korea during the launch of DUV technology in 1996–1997, to leading Cymer’s product marketing group from 1998 to 2001, researching new growth markets in the business development group in 2002, to managing chipmaker customers in the worldwide regional marketing group in 2003–2004. Prior to his appointment at Cymer, Brandt managed the engineering development, product design, and continuous product improvement activities of Chemical Vapor Deposition (CVD) systems for Watkins-Johnson. Upon the successful launch of their high-volume product, Brandt led the creation of the company’s product marketing group. Brandt holds a bachelor’s in Mechanical Engineering degree from California Polytechnic State University in San Luis Obispo, California.